INTERACTIVE JELLYFISH ANIMATION USING SIMULATION

Dave Rudolf

Department of Computer Science, University of Saskatchewan, Saskatoon, Canada
PhaseSpace Inc., San Leandro, USA

David Mould

Department of Computer Science, University of Saskatchewan, Saskatoon, Canada
School of Computer Science, Carleton University, Ottawa, Canada

Keywords: Jellyfish, Marine invertebrates, Physics-based animation, Fluid dynamics.

Abstract: This paper presents an automatic animation system for jellyfish that accounts for interaction between the organism and its surroundings. We endeavor to model the jellyfish's morphology, as well as its achieved thrust. We physically simulate the elastic body of the jellyfish and its surrounding sea water. We use a modified immersed boundary method to combine spring-mass systems and a grid-based semi-Lagrangian fluid solver. The resulting simulations are efficient with an acceptable compromise in physical accuracy. We reduce our model for axially symmetric species to 2D, and extrapolate the results to 3D. We add detail to the 3D shape with noise that is inspired by empirical observations of real jellyfish. We also suggest suitable contraction functions so that our virtual jellyfish propells itself within the water in a manner similar to the real organism. The resulting system is capable of animating jellyfish in real-time on modest desktop hardware.

1 INTRODUCTION

Seascapes are becoming more common in the computer animation industry following the popularity of productions such as Pixar's Finding Nemo (2003). As well, advances in numerical techniques and hardware are making physical simulation of virtual environments more feasible. Simulation has the advantage of automatically animating interactions between characters and their environments. This paper proposes an animation system for jellyfish that uses computational fluid dynamics so that the virtual organism can affect its environment, and vice versa.

We are interested in the unique mode of jet-propelled locomotion exhibited by jellyfish, as illustrated in Figure 1. This style of motion is largely not understood either by computer scientists or by marine biologists. Beer et al. (1997) suggest that the study of relatively simple animals such as jellyfish will yield a better idea of how to animate more complicated deformable marine life.

Physiologically, jellyfish are not overly complex: they are invertebrates with a simple nervous system (Arai, 1997). However, their mode of locomotion is still difficult to model numerically, owing to the

Figure 1: Captured footage of a real jellyfish swimming.

combination of the organism's elastic body and the surrounding incompressible fluids (Stockie & Wetton, 1999). We use simulation not for accuracy reasons, but so that our virtual jellyfish can physically interact with the water around it. Our simulations use a mass-spring system (Terzopoulos, Platt, Barr & Fleischer, 1987) to represent the elastic body of the jellyfish, and a semi-Lagrangian fluid solver (Stam, 1999) for the surrounding sea water. The two representations are coupled using the immersed boundary method (Peskin, 2002). This method is effective for our system. However, a full 3D simulation would still be quite expensive. Thus, we make reductions to our model.

Many species of jellyfish are axially symmetric, which we exploit by simulating only a low-resolution 2D slice. By doing so, we are able to animate jellyfish in an appealing, convincing, and efficient manner. We then extrapolate the 2D results to a higher resolution 3D model. Since a naïve 3D extrapolation would lack the geometric complexity seen in real jellyfish,

we also propose means to add variation back into the 3D geometry, based on observations from the biology community.

Controlling motor functions is a further challenge. Jellyfish have a simple muscular structure, but use it in complex ways that are not well studied. We give one possible approach to motor control for jellyfish, based on empirical observation. We focus on the resonant gait of jellyfish, which is marked by a regular swimming action at a rate close to a resonant frequency of the organism and its environment (Megill, 2002). We restrict our interest to fully grown adult jellyfish, as the organism most actively swims in this phase of its development.

The main contribution of this paper is our automated system for animating jellyfish, running on conventional desktop hardware at interactive rates, yet still accounting for physical interactions between the jellyfish and its surrounding fluid. Our model incorporates the biological aspects of the organism that influence its locomotion. We also show that a simulation model of jellyfish can effectively be reduced to a coarse 2D model, while providing methods to extrapolate back to a detailed and compelling 3D rendering model. We modify Peskin's immersed boundary to be more suitable for coarse models. Lastly, we also provide a simple procedural mechanism for controlling the organism's physiology in order to achieve locomotion.

Our work is most interesting to graphics researchers and tool designers. The animations produced by our model are convincing to a general audience. Although our particular model would not be accurate enough for experimental biologists, the biology community can draw inspiration from our work in developing their own simulations of jellyfish.

2 PREVIOUS WORK

Physics-based animation techniques have been developed for a wide variety of characters: snakes, worms, and caterpillars (Miller, 1988); fish (Tu & Terzopoulos, 1994); and, of course, human beings (Hodgins, Wooten, Brogan & O'Brien, 1995). Jellyfish have previously been animated through procedural techniques and key-framing (Pixar Animation Studios, 2003). These techniques do not easily model two-way interactions between the jellyfish and their environment.

Particle-based approaches such as mass-spring systems (Terzopoulos, Platt, Barr & Fleischer, 1987; Tu & Terzopoulos, 1994) can be used to simulate elastic bodies. Thus, particle-based fluid representations,

such as *smoothed particle hydrodynamics* (Desbrun & Gascuel, 1996), might seem tempting. However, SPH is not as efficient as grid-based methods (Griebel, Dornseifer & Neunhoeffer, 1998) when simulating contiguous regions of incompressible fluid, especially when large forces are acting on the fluid. Stam (1999) gives an inexpensive grid-based approach that is unconditionally stable, though with some numerical damping.

To couple particle-based solids with grid-based fluids, the graphics community typically enforces boundary conditions on the fluid that correspond to the solid surface's velocity at each fluid cell. The most recent work in this vein is that of Robinson-Mosher et al. (2008), which increases the stability of simulation by strictly enforcing conservation of momentum. From the mathematics community, Peskin (2002) uses the immersed boundary method to couple grid-based fluid representations with particle-based solids. This method is especially interesting to us because it has been used to model active elastic bodies, such as the human heart (McQueen & Peskin, 2000), that exert great force on the fluids around them. Unlike the work of Robinson-Mosher et al. (2008), the immersed boundary method does not explicitly prevent fluid from leaking across thin elastic boundaries, and performs poorly when the fluid's free surface intersects the elastic body. However, our jellyfish are completely submerged, and leakage is quite minimal (Stockie & Wetton, 1999).

As with all physics-based animation techniques, we need a way to automatically control the bodies that are in motion. For some creatures (Wu & Popović, 2003; Miller, 1988; Tu & Terzopoulos, 1994), simplified physical systems are used so that the animation has some semblance of realism, but the animation can be controlled with a relatively small number of parameters. Our system is more complex, in that it has more parameters. A more adaptive controller, such as a PID controller (Dean & Wellman, 1991), is also possible; however, tuning the weights of the control function is not a trivial task.

From the biology community, Megill (2002) discusses different gaits of jellyfish. Dabiri and Gharib (2003) provide empirical data on the large-scale morphology and kinematics of swimming jellyfish. Gladfelter (1972), and Megill (2002) describe the elastic properties of the organism, and its distribution of muscle fibres. Gladfelter also gives detailed data on the deformation of jellyfish as they contract.

The symmetry of jellyfish was previously exploited by Dabiri and Gharib (2003), though they treat the organism as perfectly symmetric. To generate a 3D model from a 2D slice, we take inspiration from

Rasmussen et al. (2003), who animated 3D explosions by augmenting the flow of 2D simulations with a 3D periodic noise field. Perlin (Perlin, 2002) gives a simple means of computing a continuous noise field.

3 A NUMERICAL MODEL OF JELLYFISH

This section describes our numerical model of jellyfish: our mass-spring configuration for of the organism's body, and how we incorporate it into a semi-Lagrangian fluid solver with a modified immersed boundary method. This section also discusses the biological aspects of the organism that are involved in its locomotion, and lastly how we extrapolate and embellish our 3D model.

3.1 Jellyfish Physiology

Figure 2 highlights the anatomy of the organism that are of interest to this work. A jellyfish swims by repeatedly contracting its umbrella, producing thrust by expelling fluid from the subumbrellar cavity. The tentacles along the aperture of the umbrella add hydrodynamic drag. These tentacles are mostly passive during normal swimming, but are used when hunting or moving along the ocean floor (Megill, 2002). Many species of jellyfish are approximately axially symmetric, where the axis of symmetry runs from the apex of the umbrella through the center of its aperture. Shih (1977) lists a large number of different species of jellyfish, whose umbrellas and tentacles vary in size and physical configuration.

Figure 2 also depicts the different tissues within the umbrella itself. The circumferential muscle that lines the subumbrellar wall is chiefly involved in locomotion. When this muscle contracts, it pulls the umbrella inward, creating a fluid jet at the aperture of the umbrella that propels the organism forward.
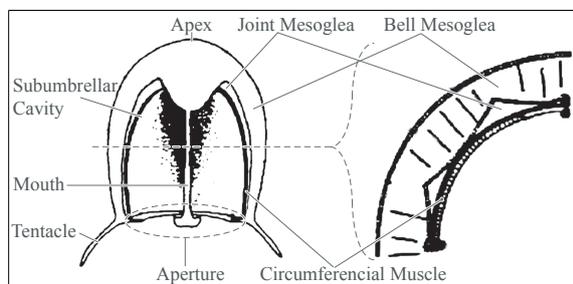

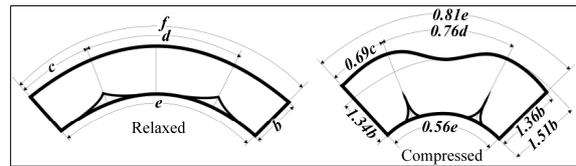Figure 2: Vertical and horizontal cross-sections of a medusan umbrella.

Figure 3: The non-linear deformation of the umbrella under the contraction of the circumferential muscle, shown as a horizontal cross-section.

Aside from the circumferential muscle, the remainder of the umbrella is categorized into two regions: the *bell mesoglea* and the *joint mesoglea*, both essentially passive. The joint mesoglea's elastic modulus is roughly 10% the bell mesoglea's, so that the when the umbrella is compressed, the joint mesoglea deforms into ridges, as illustrated in Figure 3. Because of the ridges, the elastic properties of the umbrella are not a linear function of the displacement. Megill (2002) gives us the shape of the stress-strain profile.

3.2 2D Simulation Model

We want our simulations to capture three aspects of the jellyfish's anatomy: the mesoglea; the circumferential muscle; and the tentacles. We represent the subumbrellar surface of the organism with a chain of Hookean springs, and further enforce the structure of the umbrella with angular springs. Instead of angular springs, one might be tempted to enforce relative orientations with small networks of Hookean springs, similar to the work of Miller (1988), and Tu and Terzopoulos (1994). However, we experimentally found that the large number of short springs (relative to the resolution of our fluid grid) made the system less stable. Figure 4 shows our mass-spring configuration. The circumferential muscle is represented by linear springs going longitudinally across the umbrella. These springs exert an inward thrust on the subumbrellar surface, as the circumferential muscle does in real jellyfish. To mimic a contraction of this muscle, we reduce the rest lengths of these springs to exert force on the subumbrellar wall.

Figure 4 also shows tentacles, represented by two strands of points on either side of the umbrella, connected with both linear and angular springs. The size and makeup of jellyfish tentacles can vary widely among different species and we artistically chose the physical parameters of the tentacles. We give the tentacles the same elastic modulus as the umbrella, but with 1/100th the cross-sectional area.

We model the flow of the sea water surrounding the jellyfish using the incompressible Navier-Stokes

equations:

$$\frac{\partial \vec{u}}{\partial t} = \nu \nabla^2 \vec{u} - \vec{u} \cdot \nabla \vec{u} - \frac{\nabla p}{\rho} + \vec{F}, \quad \nabla \cdot \vec{u} = 0, \quad (1)$$

where $\vec{u}$ is the fluid's velocity field, p is the pressure field, ρ is the fluid density, ν is the fluid's kinetic viscosity, $\vec{F}$ is a field of external forces acting on the fluid, and ∇ and ∇^2 respectively are spatial gradient and Laplacian operators. Griebel et al. (1998) give a thorough explanation of Equation 1.

For our 2D simulation, we use the Cartesian formulation of the Navier-Stokes equation. Since we are modeling axial symmetry, it may be tempting to use a cylindrical formulation as given by Acheson (Acheson, 1990). However, the axis of symmetry can potentially change constantly, and the two halves of the slice may not mirror each other exactly.

Sea water is essentially incompressible, and a jellyfish can exert large forces on the fluid within its cavity. Upholding the incompressibility constraint in Equation 1 is very important to our system. SPH methods (Desbrun & Gascuel, 1996) approximate incompressibility by introducing strong pressure forces between fluid particles, increasing the numerical stiffness (and thus the computational expense) of the simulation. Grid-based methods are more appropriate. We immerse our mass-spring model of the jellyfish in a square fluid volume that is ten times the jellyfish's diameter, and give the fluid cavity free-slip boundary conditions, as described by Griebel et al. (1998).

We use the immersed boundary method (Peskin, 2002) to couple the particle-based elastic and the grid-based fluid representations. In Peskin's method, the elastic point-masses are advected along the flow field of the fluid grid, and the elastic forces of the Hookean springs are applied to the fluid grid using the force term $\vec{F}$ in Equation 1. Peskin uses a smoothing kernel to distribute the forces to several, possibly dozens, of grid cells near the point-mass. Doing so increases the cost of simulation, and effectively puts an upper limit on the frequency at which the force profile can vary over the fluid grid. Since we use relatively coarse grids (i.e., 50×50 or 100×100), the frequency limitation of Peskin's smoothing kernel can make the fluid appear artificially viscous around the solid point-masses. We diverge slightly from Peskin's method, and instead distribute the elastic force of a point-mass onto its four closest grid cells with bilinear interpolation to find the contributions to each corner.

Peskin's method is known to be numerically stiff, and Stockie and Wetton (1999) show that semi-implicit integration schemes yield roughly an order of magnitude in efficiency. However, we find experimentally that we gain two orders of magnitude

in speed-up over an explicit scheme, simply by using the semi-Lagrangian method (Stam, 1999). This method does not gain us larger time-steps, but merely decreases the cost of each step. Stam's method is unconditionally stable when simulating fluids alone, but large time-steps can still make the mass-spring network unstable. Similarly, the Courant-Friedrichs-Lewy stability criterion (Griebel, Dornseifer & Neunhoeffer, 1998) does not predict time-steps that keep the elastic body stable. Lacking a better measure of stability, we controlled step sizes with the Courant-Friedrichs-Lewy condition, using a safety factor of 0.001.

3.3 Muscle Activation

Megill (2002) describes several different gaits of the jellyfish. We aim to animate the *resonant* gait, which involves an organism oscillating at or near the resonant frequency of the system. It is the most common and most studied gait.

To contract the umbrella, we modify the rest lengths of the subumbrellar springs. Biology literature provides no evidence that the organism uses closed-loop controllers such as those described by Dean (1991) to induce muscle contractions, but rather suggests a predictable, cyclical pattern (Megill, 2002; Dabiri & Gharib, 2003). We thus use Hermite splines to generate each spring's rest length over time.

When a jellyfish contracts, it propels itself forward. However, when it expands, it also pulls itself backward. For a jellyfish to achieve a net positive movement over a contraction cycle, the organism must incur less overall drag in the cycle's expansion phase than in the contraction phase. We are unaware of any literature that details how this drag reduction is achieved. We suspect that jellyfish make themselves
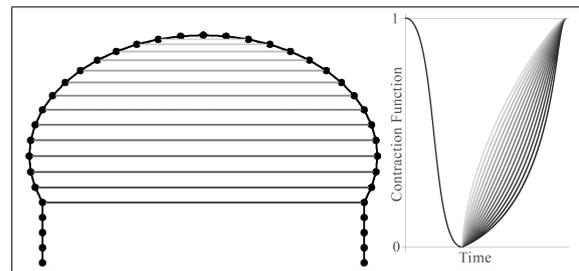

Figure 4: Our mass-spring network for a jellyfish slice, and the corresponding contraction functions that we use. Lines represent Hookean springs. Also, angular springs are used between points on the tentacles, and around the umbrella, though not across the umbrella. Each spring's greyscale level in the left image corresponds to the contraction function in the right image with the same grey level.

more flat to achieve higher drag, and more rounded to reduce their drag. In Figure 1, the first three frames show the jellyfish expanding, and its umbrella shape is relatively curved. In the fourth frame, the jellyfish is contracting, and the umbrella appears less curved and more conical. In order to achieve this morphology, we slow the expansion of subumbrellar springs close to the aperture. We give the Hermite splines for the contraction functions different slopes in the expansion phase. Springs closer to the umbrella's apex have steeper slopes than those closer to its aperture. Figure 4 shows our mass-spring model of the jellyfish, with the corresponding contraction functions for each spring.

The frequency of the jellyfish's contractions has a direct effect on the organism's achieved thrust, as well as its morphology. The resonant frequency of the system depends mostly on the umbrella's diameter (Megill, 2002). We experimented with different contraction frequencies to determine which ones were optimal for our model. Figure 5 shows the translational motion of a simulated jellyfish with an umbrella diameter of 40 mm, but with different contraction frequencies. We get a large maxima in total vertical displacement for a frequency of 0.7 Hz, which agrees with data measured by Dabiri and Gharib (2003).

3.4 3D Rendering Model

The points in our simulation model represent the subumbrellar surface. To account for the thickness of the umbrella, we generate the exumbrellar side by projecting each surface point backward along its normal. Figure 3 gives suitable thickness values. We then resample the coarse set of points to arbitrary resolutions by interpolating a cubic spline through the original point-masses and then the newly generated exumbrellar points.

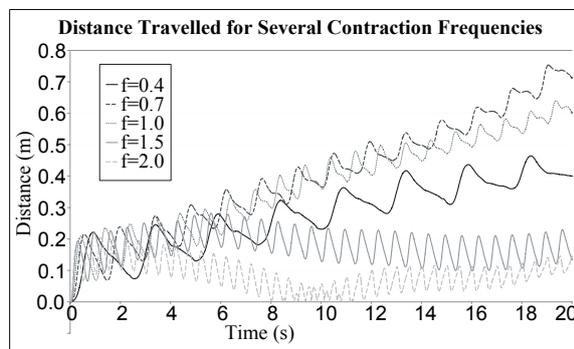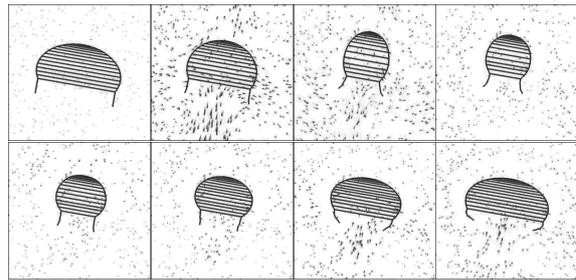The subumbrellar points may not be symmetric

Figure 6: The results of our 2D simulation; trace particles show the flow of the fluid around the contracting jellyfish.

within the 2D plane (i.e., the two sides of the umbrella may not mirror each other). Thus, we cannot extrapolate the geometry by merely rotating the results of the slice about the axis of symmetry, as Dibiri and Gharib (2003) did. Instead, we consider each pair of points $\vec{x}_i$ and $\vec{x}_j$ opposite to each other on the umbrella. Note that the pairs of points in question resulted from the resampling of the coarse geometry. We define an axis of rotation for each pair, which goes through the center of the line segment between the points $\vec{x}_i$ and $\vec{x}_j$, and is orthogonal to that line segment. We use the same disc extrapolation scheme for generating tentacles along the 3D aperture of the umbrella. Figure 7 illustrates our process of extrapolating circular area from pairs of points in our 2D model.

Our disc-based extrapolation generates an artificially smooth volume. Although a given species may be roughly symmetric, individual jellyfish are not exactly so, as seen in Figure 8. To add variation to our rendering model, we perturb each point $\vec{x}_{i,j}$ on the umbrella's surface by some scalar distance $c_{i,j}$ in the direction of its surface normal $\vec{n}_{i,j}$, where (i,j) is the azimuth and elevation indices of the point.

Several factors can cause small-scale asymmetries. Periodic features in the underlying umbrella geometry are particular to the species of jellyfish (Shih,

Figure 5: Trajectories of several simulated organisms with different frequencies of contraction.
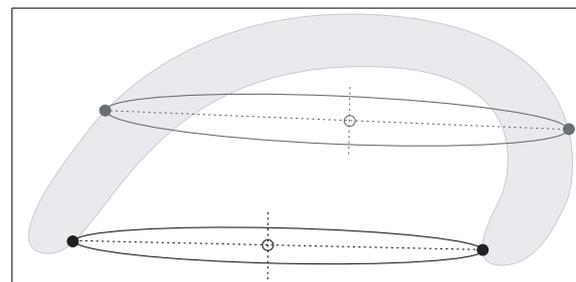

Figure 7: An example of point pairs along the 2D umbrella slice that have been extrapolated to 3D discs. For each point pair, the line between them is bisected orthoganally by the rotational axis, and a disc results from rotating those points about that axis.
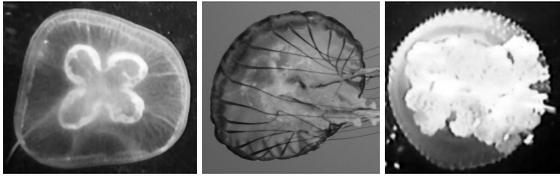
Figure 8: Jellyfish that are not exactly symmetric.

1977), as seen in the right-most two images in Figure 8. For these structural patterns, we define functions to generate the desired appearance:

$$c_{i,j}^{str} = \alpha^{str} sin(f\sigma_j), \quad \text{or} \quad c_{i,j}^{str} = \alpha^{str}|sin(f\sigma_j)|, \quad (2)$$

where α^{str} is an artistically-chosen scale factor, f is the frequency of the variation, and σ_j is the longitudinal angle of points $\vec{x}_{i,j}$ for all values of i. This angle can be expressed as:

$$\sigma_j = 2\pi\frac{j}{j_{max}}. \quad (3)$$

Another type of variation, seen in Figure 3, is caused by the nonuniform elastic properties of the jellyfish's mesoglea, which produce ripples across the contracting umbrella. This variation is also roughly sinusoidal, though its amplitude depends on the amount of umbrellar contraction. To account for contraction effects, we use a spring's uncontracted rest length l_r and its current length l_c to define a contraction coefficient that is at 1 when $l_c = l_r$, and 0 when $l_c = (0.46)l_r$. Then, the overall displacement of the umbrella hull can be described:

$$c_{i,j}^{cmp} = \alpha^{cmp}\left(\frac{l_c - \gamma l_r}{l_r - \gamma l_r}\right)\left\{\eta + \kappa\left(\frac{sin(\sigma_j) + 1}{2}\right)\right\}. \quad (4)$$

The constants $\eta = (1.34 - 1)$, $\gamma = (1 - 0.54)$, and $\kappa = (1.51 - 1.34)$ all come from Figure 3. Note that only points on the exumbrellar surface are affected in this manner.

Lastly, asymmetric differences arise between individuals of the same species. We mimic this variation artistically using Perlin noise (2002). We control the frequency of each dimension of the noise function independently, with the intent of qualitatively approximating the look of a target jellyfish. Since the mesoglea is thicker at the top of the umbrella, it is more resistant to deformation in this region. We attenuate the amplitude of the noise function for points near the peak of the umbrella. Our expression for the displacement of the umbrella points due to nonperiodic variation is as follows:

$$c_{i,j}^{noise} = \alpha^{noise}\left(\frac{i}{i_{max}}\right) * Q_P\left(\frac{2i}{i_{max}}, \frac{8j}{j_{max}}, \frac{t}{100}\right), \quad (5)$$

where t is the simulation time, and Q_P is the Perlin noise field. We apply this displacement to both subumbrellar and exumbrellar points, and also tentacle points.
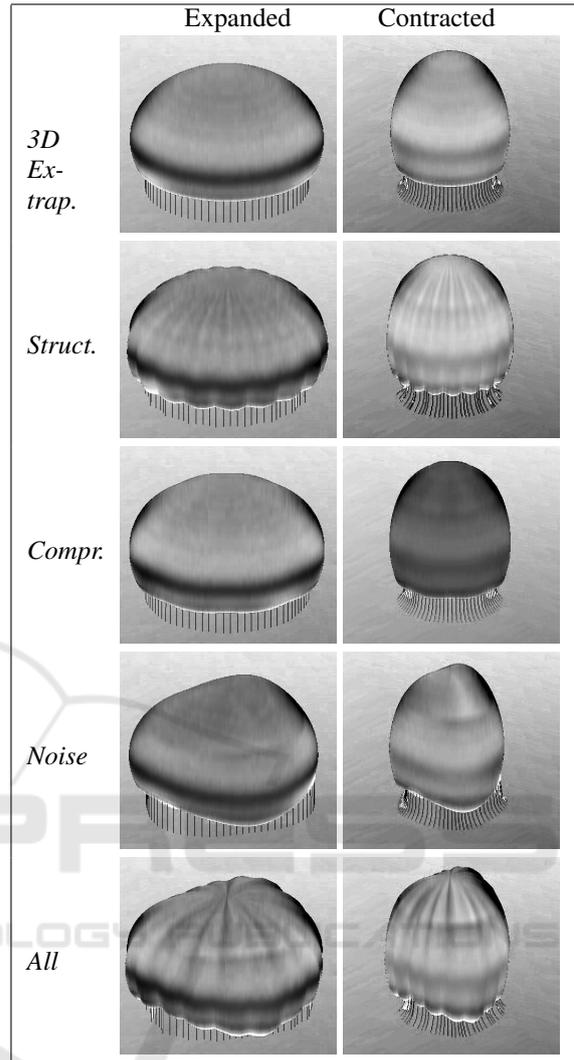

Figure 9: Our 3D extrapolation, and the types of noise that we apply to the hull of the umbrella. The first column of images shows the jellyfish at its expanded (rest) configuration, and the bottom row shows the contracted configuration.

4 RESULTS

Figure 10 shows a full cycle of our jellyfish swimming. We render the final model with a simple Lambertian surface lighting model. We find the motion of our jellyfish to be quite convincing, comparable to previous animations of jellyfish such as in Pixar's "Finding Nemo" (2003). Our method has the advantage that the resulting animation's upward movement is more closely tied to the contraction of the organism, and the virtual organism interacts with its environment directly and automatically. Also, our morphology appears to more closely resemble that of real
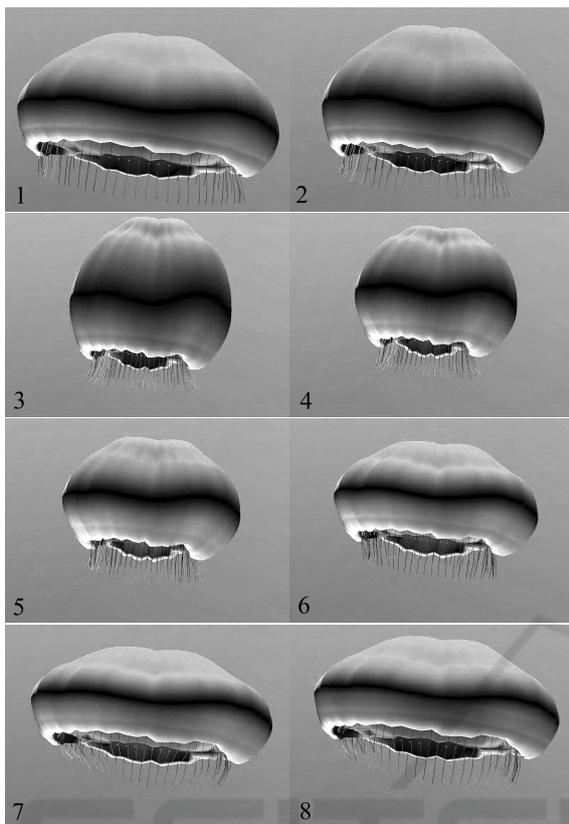
Figure 10: A sequence of frames from our animation system.

jellyfish.

Although accuracy is not the primary concern of our model, we discuss it briefly here. We found experimentally that our model has a similar resonant frequency to captured data from Dabiri and Gharib (2003). However, the motion that our model generates is noticeably different from empirical data of jellyfish. Figure 5 shows high-frequency motion that has a higher amplitude than that shown by Dabiri and Gharib (2003), meaning that our model's position oscillates up and down more, relative to its overall translational motion.

We are able to achieve real-time animations at 30 to 40 frames per second on modest hardware (AMD Turion 1.6 GHz processor), depending on the resolution of our 2D simulation and of our 3D extrapolation. We experimentally find that time-steps of the order of 0.01 seconds begin to hit the stability limits of the system. Each frame must be broken into multiple simulation steps, but of course, resampling and 3D extrapolation only needs to be done once per frame. Figure 11 shows the parameters of our simulations, and the values that we used to generate the animations that are featured in this paper.

Parameter	Value
Fluid Grid Height/Width (n)	100
Fluid Viscosity (ν)	1.304×10^{-3}
Fluid Density (ρ)	1
Safety Factor for Integration Step Size	0.001
Jellyfish Contraction Frequency	$0.7Hz$
Jellyfish Diameter	$40mm$
Jellyfish Height	$28mm$
Jellyfish Thickness (ϑ)	$4mm$
Hookean Elastic Modulus	$1186Pa$
Angular Elastic Stiffness	$1.186\,N \cdot m/rad$
Tentacle Cross-sectional Area Factor	$1/100$
Structural Variation Scale (α^{str})	$0.375 \cdot \vartheta$
Compression Variation Scale (α^{cmp})	$0.25 \cdot \vartheta$
Structural Variation Scale (α^{noise})	$2.25 \cdot \vartheta$

Figure 11: Parameters of our animation system.

5 CONCLUSIONS AND FUTURE WORK

We simulate a model of jellyfish numerically, which accounts for the elastic forces of the organism as it contracts its muscles, as well as the reaction of the sea water that surrounds the organism. Simulation allows us to model the direct interaction of the jellyfish and its environment. We simulate only a 2D vertical slice of the jellyfish and exploit the axial symmetry of the organism. We also concentrate on the resonant gait of an adult jellyfish, in which it contracts at its submerged natural resonant frequency.

We represent the jellyfish's flesh and subumbrellar muscles as a mass-spring system (Terzopoulos, Platt, Barr & Fleischer, 1987) that consists of a combination of linear and angular springs. We shorten the rest lengths of subumbrellar springs to simulate the contraction of muscles within the umbrella based on an artistically chosen periodic function. We account for sea water with a semi-Lagrangian fluid solver (Stam, 1999) in conjunction with the immersed boundary method (Peskin, 2002).

We generate a higher resolution model from our coarse simulations by threading a cubic spline interpolant around the simulated point-masses. We then extrapolate to a 3D surface by defining discs that go through either side of the jellyfish's umbrella, and add several forms of variation to the resulting 3D surface. These variations are partly based on observations of real jellyfish, and partly artistic.

Much work could still be done with respect to jellyfish animation. We would like to remove the assumption of axial symmetry, possibly by simulating multiple 2D slices. Also, jellyfish are capable of other locomotion modes besides the common resonant gait, and simulating these would increase the range of motion of our virtual jellyfish.

We still know little about exactly how jellyfish contract their muscles to achieve jet propulsion. Van de Panne and Fiume (1993) designed a means of experimenting with the control processes for simple creatures using sensor-actuator networks. We could perhaps leverage this kind of control exploration within the context of jellyfish.

In our work, we have not discussed how some species of jellyfish are able to reorient themselves. Megill (2002) states that there are sparse muscle fibres in the bell mesoglea that are normal to the umbrella's surface. These fibres can change the symmetry of the umbrella and thus effect a course change for the organism as it swims, though the exact process is not well understood. So far, we were not able to reproduce this phenomenon within our model.

We could improve our rendering of the jellyfish by considering translucence and bioluminescence, and by improving our noise model. Also, our rendering model currently lacks the venous structure visible in some species of jellyfish.

REFERENCES

Acheson, D. J. (1990). *Elementary Fluid Dynamics*. Oxford: Oxford University Press.

Arai, M. N. (1997). *A Functional Biology of Scyphozoa*. London: Chapman and Hall.

Beer, R. D., Quinn, R. D., Chiel, H. J., & Ritzmann, R. E. (1997). Biologically inspired approaches to robotics: what can we learn from insects? *Commun. ACM*, *40*(3), 30–38.

Dabiri, J. O. & Gharib, M. (2003). Sensitivity analysis of kinematic approximations in dynamic medusan swimming models. *Journal of Experimental Biology*, *206*, 3675–3680.

Dean, T. & Wellman, M. (1991). *Planning and Control*. San Francisco: Morgan Kaufmann Publishers.

Desbrun, M. & Gascuel, M.-P. (1996). Smoothed particles: a new paradigm for animating highly deformable bodies. In *Proceedings of the Eurographics workshop on Computer animation and simulation '96*, (pp. 61–76)., New York, NY, USA. Springer-Verlag New York, Inc.

Gladfelter, W. B. (1972). Structure and function of the locomotory system of polyorchis montereyensis (cnidaria, hydrozoa). *Helgolaender Wiss. Meeresunters*, *23*, 38–79.

Griebel, M., Dornseifer, T., & Neunhoeffer, T. (1998). *Numerical Simulation in Fluid Dynamics: a practical introduction*. Philadelphia: Society for Industrial and Applied Mathematics.

Hodgins, J. K., Wooten, W. L., Brogan, D. C., & O'Brien, J. F. (1995). Animating human athletics. In *Proceedings of SIGGRAPH '95*, (pp. 71–78). ACM Press.

McQueen, D. M. & Peskin, C. S. (2000). Heart simulation by an immersed boundary method with formal second-order accuracy and reduced numerical viscosity. In *Mechanics for a New Millennium: Proceedings of the International Conference on Theoretical and Applied Mechanics (ICTAM)*, (pp. 429–444).

Megill, W. M. (2002). The biomechanics of jellyfish swimming. Ph.D. Dissertation, Department of Zoology, University of British Columbia.

Michiel van de Panne, E. F. (1993). Sensor-actuator networks. In *Proceedings of SIGGRAPH '93*, (pp. 335–342)., New York, NY, USA. ACM Press.

Miller, G. S. P. (1988). The motion dynamics of snakes and worms. In *Proceedings of SIGGRAPH '88*, (pp. 169–173). ACM Press.

Perlin, K. (2002). Improving noise. In *Proceedings of SIGGRAPH '02*, (pp. 681–682)., New York, NY, USA. ACM Press.

Peskin, C. (2002). The immersed boundary method. *Acta Numerica 11*, 479–517.

Pixar Animation Studios, W. D. P. (2003). Finding Nemo motion picture. DVD.

Rasmussen, N., Nguyen, D. Q., Geiger, W., & Fedkiw, R. (2003). Smoke simulation for large scale phenomena. *ACM Trans. Graph.*, *22*(3), 703–707.

Robinson-Mosher, A., Shinar, T., Gretarsson, J., Su, J., & Fedkiw, R. (2008). Two-way coupling of fluids to rigid and deformable solids and shells. In *SIGGRAPH '08: ACM SIGGRAPH 2008 papers*, (pp. 1–9)., New York, NY, USA. ACM.

Shih, C. T. (1977). *A Guide to the Jellyfish of Canadian Atlantic Waters*. Number 5. Ottawa, Canada: National Museum of Natural Sciences.

Stam, J. (1999). Stable fluids. In *Proceedings of SIGGRAPH '99*, (pp. 121–128)., New York, NY, USA. ACM Press/Addison-Wesley Publishing Co.

Stockie, J. M. & Wetton, B. R. (1999). Analysis of stiffness in the immersed boundary method and implications for time-stepping schemes.

Terzopoulos, D., Platt, J., Barr, A., & Fleischer, K. (1987). Elastically deformable models. In *Proceedings of SIGGRAPH '87*, (pp. 205–214). ACM Press.

Tu, X. & Terzopoulos, D. (1994). Artificial fishes: Physics, locomotion, perception, behavior. *Computer Graphics*, *28*(Annual Conference Series), 43–50.

Wu, J. & Popović, Z. (2003). Realistic modeling of bird flight animations. *ACM Trans. Graph.*, *22*(3), 888–895.